Am. Chem. Soc. 106, 765–784.
Weiner, S. J., Kollman, P. A., Nguyen, D. T., & Case, D. A. (1986) J. Comput. Chem. 7, 230–252.
Willumsen, B. M., Adari, H., Zhang, K., Papageorge, A. G., Stone, J. C., McCormick, F., & Lowy, D. R. (1989) in The Guanine Nucleotide Binding Proteins, NATO ASI Series A, Vol. 165, pp 165–177, Plenum, New York.
Yamasaki, K., Kawai, G., Ito, Y., Muto, Y., Fujita, J., Miyazawa, T., Nishimura, S., & Yokoyama (1989) Biochem. Biophys. Res. Commun. 162, 1054–1062.

Crystal Structure of an Electron-Transfer Complex between Methylamine Dehydrogenase and Amicyanin[†,‡]

Longyin Chen,[§] Rosemary Durley,[§] Barbara J. Poliks,[§] Kensaku Hamada,[§] Zhiwei Chen,[§] F. Scott Mathews,*[,§] Victor L. Davidson,[∥] Yoshinori Satow,[⊥] Eric Huizinga,[#] Fred M. D. Vellieux,[#] and Wim G. J. Hol[#]

Department of Cell Biology and Physiology, Washington University School of Medicine, St. Louis, Missouri 63110, Department of Biochemistry, University of Mississippi Medical Center, Jackson, Mississippi 39216, Photon Factory, National Laboratory for High-Energy Physics (KEK), Tsukuba, Ibaraki 305, Japan, and Bioson Research Institute, University of Groningen, 9747 AG Groningen, The Netherlands

Received February 11, 1992; Revised Manuscript Received March 24, 1992

ABSTRACT: The crystal structure of the complex between the quinoprotein methylamine dehydrogenase (MADH) and the type I blue copper protein amicyanin, both from *Paracoccus denitrificans*, has been determined at 2.5-Å resolution using molecular replacement. The search model was MADH from *Thiobacillus versutus*. The amicyanin could be located in an averaged electron density difference map and the model improved by refinement and model building procedures. Nine β-strands are observed within the amicyanin molecule. The copper atom is located between three antiparallel strands and is about 2.5 Å below the protein surface. The major intermolecular interactions occur between amicyanin and the light subunit of MADH where the interface is largely hydrophobic. The copper atom of amicyanin and the redox cofactor of MADH are about 9.4 Å apart. One of the copper ligands, His 95, lies between the two redox centers and may facilitate electron transfer between them.

Many methylotrophic bacteria, when grown on methylamine as the sole source of carbon and energy, synthesize a soluble periplasmic methylamine dehydrogenase (MADH)[1] (de Beer et al., 1980). MADH catalyzes the oxidative deamination of primary amines and donates electrons to one or more *c*-type cytochromes, through a mediating blue copper protein called amicyanin (Husain & Davidson, 1985, 1986).

MADH is a heterotetramer consisting of two identical heavy (H) and two identical light (L) subunits. The enzyme from *Paracoccus denitrificans* (PD-MADH) has subunit molecular masses of 46.7 and 15.5 kDa, respectively (Husain & Davidson, 1987). The redox cofactor of MADH has been shown to be tryptophan tryptophylquinone (TTQ, Figure 1), which is composed of a pair of posttranslationally modified tryptophan residues of the L subunit which are cross-linked and contain an *o*-quinone group on one of them (McIntire et al., 1991; Chen et al., 1991).

To date no complete amino acid sequence of MADH from any source has been reported. The amino acid sequence (Ishii et al., 1983) and DNA sequence (Chistoserdov et al., 1990) of the L subunit of the enzyme from *Methylobacterium extorquens* AM1 (formerly called *Pseudomonas* AM1) have been determined. The crystal structure of MADH from *Thiobacillus versutus* (TV-MADH) has been reported recently and an amino acid sequence deduced from the electron density at 2.25-Å resolution of both the H and L subunits (Vellieux et al., 1989, 1990). The latter structure was used as the search model for molecular replacement to solve the crystal structure of MADH from *P. denitrificans* (Chen et al., 1992).

The amino acid sequence of the amicyanin of *P. denitrificans* has been determined (van Spanning et al., 1990), and the protein was shown to have a molecular mass of 12.5 kDa. Most of the physical, redox, and spectroscopic properties of amicyanin are very similar to those of other small blue copper proteins such as azurin and plastocyanin. Available amino acid sequence data indicate that amicyanins are a separate and unique class of copper proteins bearing closest similarity with plastocyanin (van Beeumen et al., 1991). Resonance Raman spectroscopic studies (Sharma et al., 1988) and two-dimensional NMR studies (Lommen et al., 1988) support this claim.

The specificity of interaction between amicyanin and MADH has been best demonstrated by studies of the proteins isolated from *P. denitrificans*. Each of these proteins is induced in this bacterium only during growth on methylamine

[†] This work is supported by NSF Grant DMB-8816618 and USPHS Grant GM41574 and by the Netherlands Foundation for Chemical Research (SON) with financial aid from the Netherlands Organization for Scientific Research (NWO).

[‡] Crystallographic coordinates have been deposited in the Brookhaven Protein Data Bank under the file name IMDA.

* To whom correspondence should be addressed.
[§] Washington University School of Medicine.
[∥] University of Mississippi Medical Center.
[⊥] National Laboratory for High-Energy Physics (KEK).
[#] University of Groningen.

[1] Abbreviations: MADH, methylamine dehydrogenase; PD-MADH, *Paracoccus denitrificans* methylamine dehydrogenase; rms, root mean square; TV-MADH, *Thiobacillus versutus* methylamine dehydrogenase; TTQ, tryptophan tryptophylquinone.

0006-2960/92/0431-4959$03.00/0

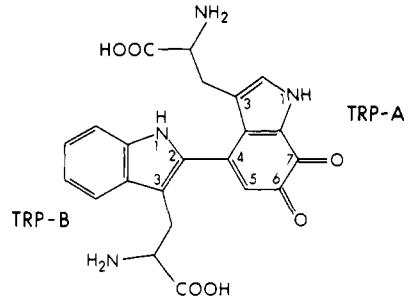

FIGURE 1: Tryptophan tryptophylquinone (TTQ). Trp-A and Trp-B correspond to positions 57 and 107 of the L subunit of MADH.

as the sole carbon source (Husain & Davidson, 1985, 1987). Furthermore, the amicyanin gene is located immediately downstream of that for the small subunit of MADH, and inactivation of the former by means of gene replacement results in complete loss of the ability to grow on methylamine (van Spanning et al., 1990).

Complex formation between MADH and amicyanin causes perturbation of the absorption spectrum of TTQ and a −73-mV shift in the redox potential of the copper center of amicyanin (Gray et al., 1988). This shift in potential is critical because it facilitates an otherwise thermodynamically unfavorable electron transfer from free amicyanin (E_m = 295 mV) to cytochrome c_{551i} (E_m = 190 mV). The complex between MADH and amicyanin has been further characterized by steady-state kinetic analysis (Davidson & Jones, 1991), chemical cross-linking studies (Kumar & Davidson, 1990), and resonance Raman spectroscopy (Backes et al., 1991). Kinetic studies indicated that the K_m value for amicyanin as an electron acceptor for MADH increased 10-fold on addition of 0.2 M NaCl, suggesting a role for electrostatic interactions in stabilizing complex formation. Chemical cross-linking studies of these proteins suggested that complex formation was stabilized in part by hydrophobic interactions between the large subunit of MADH and amicyanin and by a combination of hydrophobic and electrostatic interactions between the small subunit and amicyanin. Resonance Raman studies revealed no change in the spectra of either the protein-bound TTQ or copper upon complex formation, suggesting that no structural change in either site had occurred and that the observed perturbations in the absorption spectrum of TTQ and the redox potential of amicyanin were probably due to long-range electrostatic effects.

Experimental Procedures

Crystals of the complex between MADH and amicyanin, both isolated from *P. denitrificans*, were grown by vapor diffusion against 2.4 M sodium/potassium phosphate buffer, pH 6.5 (Chen et al., 1988). The complex is a heterohexamer composed of three types of subunits, the heavy (H) and light (L) subunits of MADH and amicyanin (A). The crystals are tetragonal, space group $P4_12_12$, with cell parameters a = 124.6 Å and c = 247.3 Å, and contain one heterohexamer of about 150 kDa per asymmetric unit. Crystals of the complex between MADH and copper-free apoamicyanin were prepared under identical conditions.

Initial data collection from several crystals of the complex between MADH and amicyanin, and of the isomorphous complex between MADH and apoamicyanin, was carried out using image plates at the synchrotron facilities of the Photon Factory in Japan. The raw data from imaging plates were processed using a modified version of the film-scanning program DENZO (Otwinowski, personal communication) and merged into discrete data sets using the crystallographic computing package ROCKS (Reeke, 1984) as adapted for the VAX computer (Bethge, 1984). Because some of the plates were badly overexposed, neither the holo nor the apo data sets were more than 77% complete at 3.0-Å resolution, and the number of reflections in common to the two data sets was only about 60%. However, a nearly complete data set could be obtained by combining the data from both types of crystals, which differ by only 2 atoms of copper of a total of about 10 000 non-hydrogen atoms. For the combined synchrotron data the R_{merge} was 8.4% to 3.0-Å resolution, where R_{merge} is defined as $R_{merge} = \sum|I - \bar{I}|/\sum I$, summed over all reflections, and I is the intensity. Further data collection from the holoamicyanin complex was carried out using the area detector facility at the University of California at San Diego (UCSD). The UCSD data were recorded from six crystals and combined into a single data set (Howard et al., 1985) which is about 83% complete to 2.5-Å resolution. For the UCSD data, R_{merge} = 8.3% to 2.5-Å resolution.

The position and orientation of the H_2L_2 portion of the complex were determined unambiguously by molecular replacement with MERLOT (Fitzgerald, 1988) using the synchrotron data and the heterotetramer of TV-MADH as the search probe (Vellieux et al., 1989, 1990). Data between 8 and 4 Å in resolution were used and the Patterson search radius was 23.5 Å. The largest peak in the rotation function was 2.9 times the rms value of the function while the second highest peak was 85% as large. The translation function gave a single peak in each of three Harker sections with secondary peaks all below 70% of the major ones. An R-factor search, where $R = \sum|F_o - F_c|/\sum F_o$, summed over all reflections, and F_o and F_c are the observed and calculated structure factors, respectively, was also carried out. The lowest value of R = 50.9% corresponded to the translation function result. Rigid body refinement yielded an R-factor of 43.7%, also in the same resolution range. Restrained refinement with PROLSQ (Hendrickson & Konnert, 1980) gave an R-factor of 41.5% from 10- to 2.75-Å resolution.

In order to locate the copper atoms, a difference Fourier was calculated at 3.0-Å resolution between the holo and the apo complex data sets. The H_2L_2 tetramer of MADH, excluding TTQ, was used in the structure factor calculation. The highest peak lay just outside of the molecular boundary of MADH and was strongly suspected to be one of the copper positions. The peak at the site related by the molecular symmetry of MADH was considerably lower. The copper positions subsequently turned out to be correct.

Since the synchrotron data were less complete than the UCSD data at higher resolution and had poorer internal agreement, subsequent analysis utilized the UCSD data. Restrained refinement of the MADH tetramer alone gave an R-factor of 38% (10–2.5-Å resolution). The $(F_o - F_c)$ difference map showed both copper atoms lying in strong electron density, with the second site about 80% as high as the first. In addition, the electron density for the cofactor of MADH corresponded well to the model of TTQ (Figure 2). Using plastocyanin (Guss & Freeman, 1983) as a guide, residues 21–105 of amicyanin could be traced in the difference map after it had been averaged about the molecular 2-fold axis (Bricogne, 1976). For the averaging, the molecular symmetry transformation matrix was obtained by superimposing the C_α positions of both pairs of subunits of MADH using the program HOMO (Argos & Rossmann, 1975). Subsequent rebuilding of the amicyanin portion of the complex and refinement of the complex using TNT (Tronrud et al., 1987) with residues 21–105 of amicyanin and the TTQ cofactor included

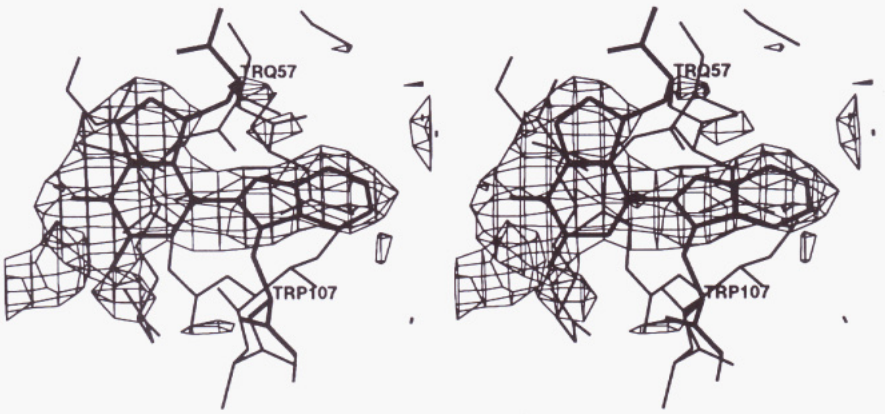

FIGURE 2: Difference electron density ($F_o - F_c$) of the MADH–amicyanin complex corresponding to the site of TTQ in one of the L subunits of MADH. The density is contoured at about two times the rms difference density. The map was computed after refinement of the starting model of MADH obtained by molecular replacement against the UCSD data to an *R*-factor of 0.38 as described in the text. TTQ was not included, and the two tryptophans at positions 57 and 107 were replaced by alanine for this calculation.

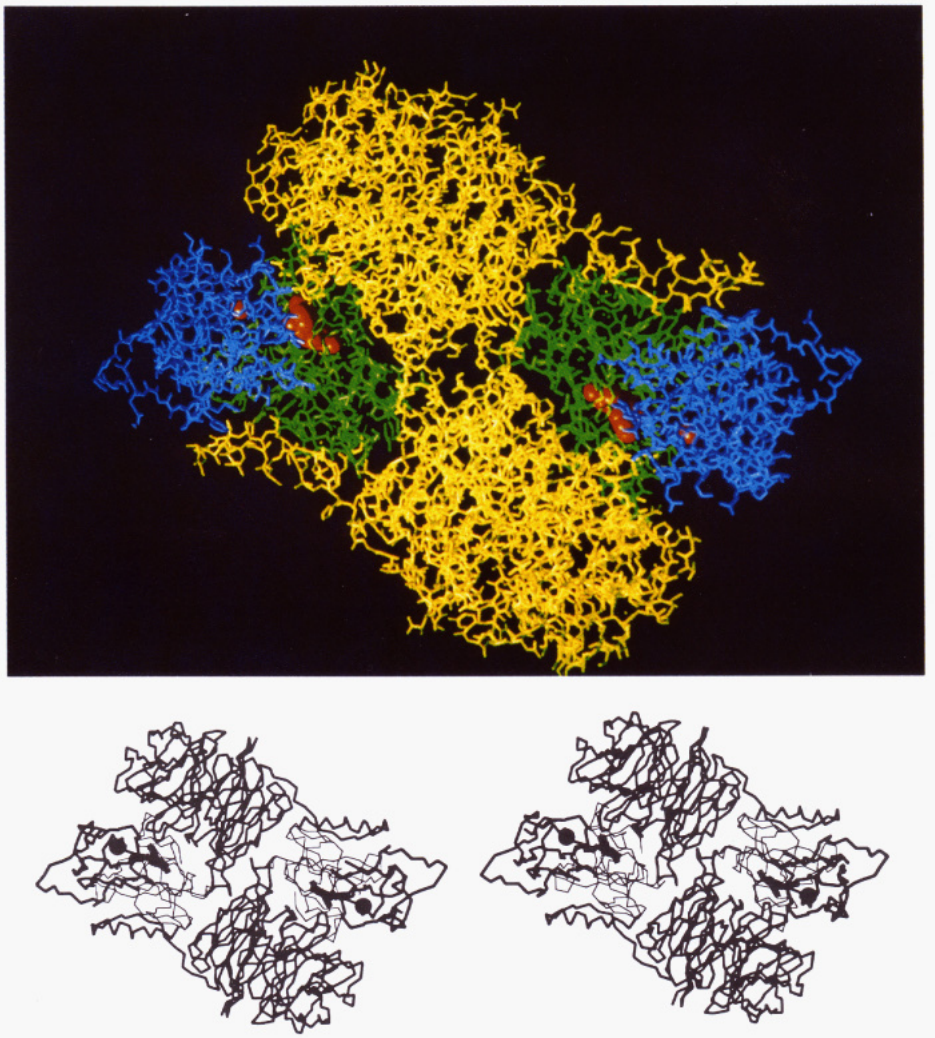

FIGURE 3: Heterohexamer of the MADH–amicyanin complex. (a, top) The $H_2L_2A_2$ hexamer of the complex contains two amicyanin molecules (in blue) attached to MADH. Each one interacts with an L subunit (in green) and to a lesser extent with an H subunit (in yellow). The TTQ cofactors and the copper atoms are shown in red. (b, bottom) Stereo diagram of the C_α backbone of the complex. The L subunits are drawn in thin lines, and the H subunits (top and bottom subunits) and amicyanin molecules (left and right subunits) are drawn in thick lines. The copper atoms and TTQ prosthetic groups are also shown.

in the model reduced the *R*-factor to 31.0%. For this and subsequent refinement and model building no additional 2-fold averaging was carried out.

A new ($F_o - F_c$) difference map indicated positions for residues 4–20 of amicyanin, consistent with weak density in the averaged map, which were included in subsequent refinement. At this point, two major refinement stages were carried out with TNT consisting of ten cycles of positional refinement followed by three cycles of thermal factor refinement. In between the two stages of refinement, both models of amicyanin were refitted to a ($2F_o - F_c$) difference map on the graphics system. No refitting of the MADH portion of

the complex was carried out since the true amino acid sequence was not known. In the second refinement stage, restraints on the Cu–ligand bond distances and the cross-link between the indole rings of TTQ were introduced to prevent distortion of the structure. Numerical values for the Cu–ligand restraints were taken from those observed in plastocyanin (Guss & Freeman, 1983). At the end of refinement, the *R*-factor was 28.5% with rms deviations from ideal bond lengths and angles of 0.015 Å and 3.2°, respectively. The average thermal factors were about 25 Å^2 for the MADH models and about 45 Å^2 for the amicyanin models. No water molecules were included in the refinement. Further refinement will be postponed until the true amino acid sequence of PD-MADH becomes available.

Results and Discussion

The complex of MADH with amicyanin consists of a heterohexamer of the type $H_2L_2A_2$ as shown in Figure 3. The H_2L_2 unit corresponds to the H_2L_2 tetramer of MADH reported previously (Vellieux et al., 1989; Chen et al., 1992). This tetramer can most easily be described as a dimer of HL dimers with strong subunit interactions within the HL dimer and weaker interactions between dimers. Each amicyanin molecule is in contact with both H and L subunits of a single HL dimer. The most extensive interactions are between amicyanin and the L subunit.

The structure of the MADH portion of the complex is virtually the same as that of the TV- and PD-MADH molecules determined previously (Vellieux et al., 1989; Chen et al., 1992). Each H subunit consists of a disk-shaped domain composed of seven four-stranded antiparallel β-sheets arranged in pseudo-7-fold symmetry, preceded by a 31-residue extended arm. Each L subunit contains ten antiparallel β-strands and six disulfide cross-links. Of particular importance is the fact that the electron density for the TTQ cofactor (Figure 2), which was not included in the calculation of structure factors for the complex in the early stages of refinement, is consistent with the shape of TTQ (Chen et al., 1991). Also, the N-terminal arm of the H subunit appears to be intact, in contrast to that of the uncomplexed crystalline PD-MADH (Chen et al., 1992), which undergoes proteolytic degradation of the first 18 residues during crystallization.

The current model of amicyanin consists of 102 residues, corresponding to positions 4–105 of the amino acid sequence. A ribbon drawing of the amicyanin backbone is shown in Figure 4. The backbone forms a nine-stranded β-sandwich topologically similar to plastocyanin (Guss & Freeman, 1983). The β-sandwich of amicyanin consists of a four-stranded mixed β-sheet facing a five-stranded mixed β-sheet. Strand 1 forms the outside strand of the four-stranded sheet and is absent in plastocyanin.

The interior of amicyanin is hydrophobic while the surface is relatively polar. The copper atom is located close to one end of the molecule near the top in Figure 4. There are four ligands to the copper atom, His 53, Cys 92, His 95, and Met 98. The pattern of copper ligation is similar to that found in plastocyanin (Guss & Freeman, 1983) and azurin (Baker, 1988) as predicted from the amino acid sequence when compared to other copper proteins (van Spanning et al., 1990). His 53 is located near the N-terminal end of β-strand 5 while the remaining ligands are located on a loop connecting strands 8 and 9. Figure 5 shows the copper and the four ligand residues superimposed on the electron density. The copper ligands are arranged approximately as a tetrahedron. Three of the ligands are buried within the protein but a fourth, His 95, lies on the protein surface, with its N$^\delta$ nitrogen atom bound

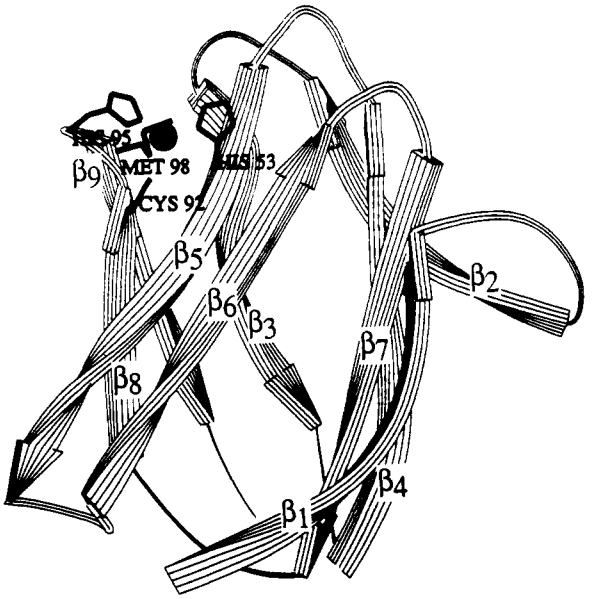

FIGURE 4: Ribbon diagram of amicyanin in the MADH–amicyanin complex. The overall structure is a nine-stranded β-barrel which is folded into two mixed β-sheets, a four-stranded sheet (strands 1, 7, 4, 2) facing a five-stranded sheet (strands 6, 5, 8, 9, 3). The copper is located at one end of the molecule (the so-called northern end). One copper ligand, His 53, is located on strand 5, while the others, Cys 92, His 95, and Met 98, are in the loop region between strands 8 and 9.

to the copper and its N$^\epsilon$ atom exposed to the surface.

Surrounding His 95 on the protein surface is a cluster of seven hydrophobic residues which together form a patch. This patch includes three Met, three Pro, and one Phe in addition to His 95, with the copper atom just underneath (Figure 6). Upon complex formation, each amicyanin molecule loses approximately 600 Å^2 of accessible surface area (Kabsch & Sander, 1983). About 375 Å^2 (63%) of this area is contained in this patch. Approximately 12 nonpolar or neutral side chains on the MADH molecule are involved in the interface with each amicyanin according to the X-ray sequence from TV-MADH. Three of these are on the H subunit and nine on the L subunit. Included in the latter is the Trp 107 moiety of the TTQ cofactor. However, detailed identification of these residues is uncertain since the complete sequence of PD-MADH has not been reported.

The relative positions of the TTQ cofactor and the copper atom of amicyanin are shown in Figure 7. The TTQ is oriented so that the *o*-quinol portion of Trp 57 is pointed away from the copper atom while the Trp 107 portion lies closest to the copper, with its indole moiety exposed at the surface of the L subunit and facing the copper region of amicyanin. The closest approach of the TTQ to the copper atom, about 9.3 Å, is from the C$^{\eta 2}$ portion of Trp 107. Thus, the active site of MADH, centered on the *o*-quinol of Trp 57 of the TTQ is located quite far from the amicyanin binding site, allowing substrate binding and product release to occur without interfering with the electron transfer to the copper atom.

His 95 of amicyanin, one of the copper ligands, is situated between the copper and the TTQ group. The closest distance between the two groups is about 5.4 Å, from C$^\delta$ of His 95 of amicyanin (residue 5095 in Figure 7) to C$^{\eta 2}$ of the Trp 107 portion of TTQ in the MADH L subunit (residue 2107 in Figure 7). Thus, His 95 of amicyanin is in a good position to mediate the electron transfer.

The presence of a histidine residue surrounded by a surface hydrophobic patch analogous to His 95 of amicyanin is a

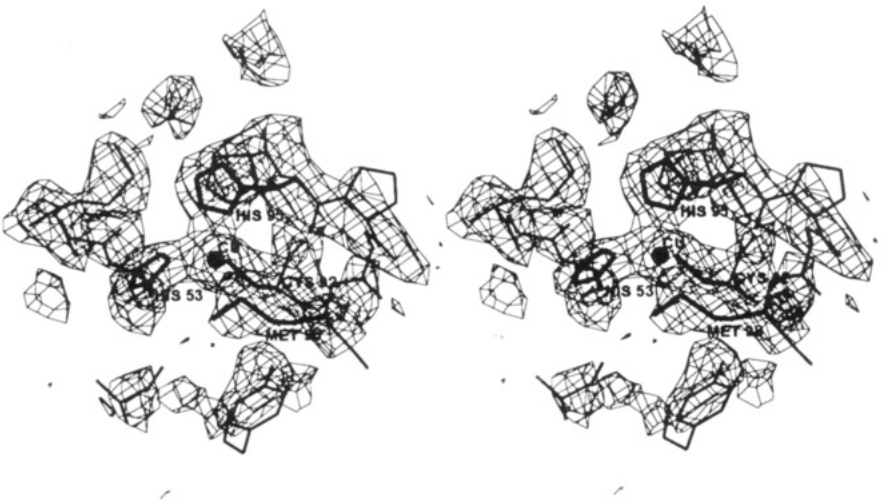

FIGURE 5: Final electron density of the MADH–amicyanin complex centered on the copper atom of one of the two independent molecules of amicyanin (subunit A_1). For purposes of illustration, an "omit" map was calculated in which the copper as well as 13 residues around the copper was excluded from the phase calculation. The contour level corresponds to about two times the rms difference density. The side chains of the four copper ligands are drawn in thick lines.

FIGURE 6: The hydrophobic surface of amicyanin at the amicyanin–MADH interface region. In the diagram, His 95 sits in the center and the copper is located underneath. Around His 95 is a highly nonpolar ring consisting of seven residues.

conserved feature of azurin and plastocyanin (Baker, 1988; Guss & Freeman, 1983). It has long been speculated that this region may be involved in mediating electron transfer to copper (Farver & Pecht, 1991). Support for this view is provided by studies of electron self-exchange rates (Groeneveld, 1988) and by mutagenesis (van der Kamp, 1991) of azurin. The present data provide direct evidence that this is true.

That Trp 107 is exposed on the surface of MADH and lies close to His 95 of amicyanin implies that it may be involved in mediating electron transfer to this His from the *o*-quinone of Trp 57. Although the planes of the two tryptophan residues in TTQ are inclined by about 45°, electron transfer through Trp 107 to His 95 of amicyanin is likely to be much more efficient than through-space electron transfer directly from Trp 57 (Beratan et al., 1990).

Electrostatic interactions have long been thought to play a critical role in stabilizing protein–protein interactions between soluble redox partners. For amicyanin and MADH, it was previously observed that the degree of cross-linking between them (Kumar & Davidson, 1990) and the complex-dependent changes in the absorption spectrum of TTQ and in the redox potential of amicyanin (Gray et al., 1988), as well as the kinetic efficiency (Davidson & Jones, 1991) of this complex, are sensitive to ionic strength in a manner that suggests a role for electrostatic interactions. However, the current data indicate that many of the interactions which stabilize this complex are hydrophobic. Given these structural results, an important question to be addressed in subsequent studies is the nature of the molecular interactions between amicyanin and MADH which can account for these observed ionic strength dependent phenomena. Further, the underlying cause of the −73-mV

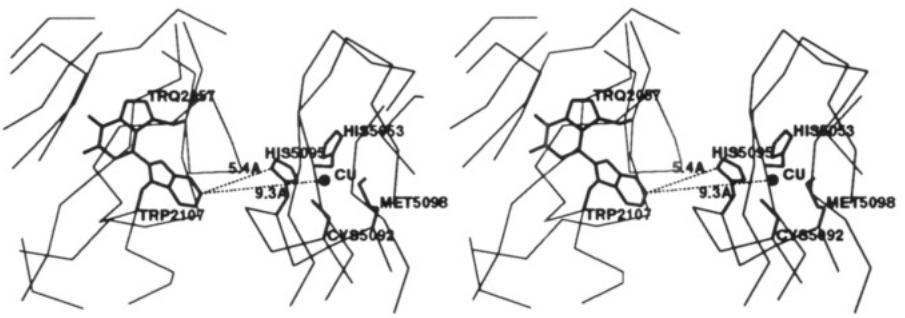

FIGURE 7: The amicyanin–MADH interface. Relative positions and distances between TTQ and the copper ligand are shown. The side chains of only the TTQ and the copper ligands are shown. All other residues are shown as CA backbone. The H subunit is omitted for clarity. The *o*-quinol portion of TTQ (Trp 57, labeled 2057) is pointed away from the interface while the indole moiety of Trp 107 (labeled 2107) is exposed to the interface. The copper is buried in amicyanin. His 95 (labeled 5095) is situated between TTQ and copper.

redox potential shift of amicyanin (Gray et al., 1988) which attends complex formation remains to be determined.

Since the complex was crystallized in high salt, one would expect such conditions to favor hydrophobic and deter hydrophilic interactions. It is not surprising then that we see primarily hydrophobic interactions in the structure. Oppositely charged groups which may normally interact in solution may not be oriented in the same manner in the crystalline complex but may point away from each other. However, this would not necessarily mean that the orientation of TTQ and copper and the path between them are any different in this structure. While we cannot exclude the possibility that this structure is not identical to that which is truly required for electron transfer, it would seem at worst to be a very close approximation. We consider the present results to provide a working model; additional biochemical studies as well as better refined structural information will be required to absolutely prove its validity.

The most significant aspect of the MADH–amicyanin complex structure is the arrangement of the two electron-transfer partners. Although two other structures of intermolecular electron-transfer complexes are known, namely, the photosynthetic reaction center (Deisenhofer et al., 1984) and *p*-cresol methylhydroxylase (Mathews et al., 1991), this is the first structure of such a complex between partners which associate weakly in solution. It is also the first structural example of a copper protein or quinoprotein involved in a complex. The copper and TTQ atoms are separated by a reasonable distance for efficient electron transfer, consistent with that observed in other inter- and intramolecular electron-transfer complexes (Deisenhofer et al., 1984; Mathews et al., 1991; Xia et al., 1990). Electron transfer appears to be mediated by a histidine side chain, which is liganded to copper. The intermolecular recognition and interaction site appears to be mainly hydrophobic in nature, consistent with certain observations from solution studies.

References

Backes, G., Davidson, V. L., Huitema, F., Duine, J. A., & Sanders-Loehr, J. (1991) *Biochemistry 30*, 9201–9210.

Baker, E. N. (1988) *J. Mol. Biol. 203*, 1071–1095.

Beratan, D. N., Onuchic, J. N., Betts, J. N., Bowler, B. E., & Gray, H. B. (1990) *J. Am. Chem. Soc. 112*, 7915–7921.

Bethge, P. H. (1984) *J. Appl. Crystallogr. 17*, 215.

Chen, L., Lim, L. W., Mathews, F. S., Davidson, V. L., & Husain, M. (1988) *J. Mol. Biol. 203*, 1137–1138.

Chen, L., Mathews, F. S., Davidson, V. L., Huizinga, E. G., Vellieux, F. M. D., Duine, J. A., & Hol, W. J. G. (1991) *FEBS Lett. 287*, 163–166.

Chen, L., Mathews, F. S., Davidson, V. L., Huizinga, E. G., Vellieux, F. M. D., & Hol, W. J. G. (1992) *Proteins* (in press).

Chistoserdov, A. Y., Tsygankov, Y. D., & Lidstrom, M. E. (1990) *Biochem. Biophys. Res. Commun. 172*, 211–216.

Davidson, V. L., & Jones, L. H. (1991) *Anal. Chim. Acta 249*, 235–240.

de Beer, R., Duine, J. A., Frank, J., & Large, P. J. (1980) *Biochim. Biophys. Acta 622*, 370–374.

Deisenhofer, J., Epp, O., Miki, K., Huber, R., & Michel, H. (1984) *J. Mol. Biol. 180*, 385–398.

Farver, O., & Pecht, I. (1991) *FASEB J. 5*, 2554–2559.

Fitzgerald, P. M. D. (1988) *J. Appl. Crystallogr. 21*, 273–278.

Gray, K. A., Davidson, V. L., & Knaff, D. B. (1988) *J. Biol. Chem. 263*, 13987–13990.

Groeneveld, C. M., Ouwerling, M. C., Erkelens, C., & Canters, G. W. (1988) *J. Mol. Biol. 200*, 189–199.

Guss, J. M., & Freeman, H. C. (1983) *J. Mol. Biol. 169*, 521–563.

Hendrickson, W. A., & Konnert, J. H. (1980) in *Biomolecular Structure, Function, Conformation and Evolution* (Srinivasan, R., Ed.) Vol. 1, pp 43–57, Pergamon, Oxford, England.

Howard, A. J., Nielsen, C., & Xuong, Ng. H. (1985) *Methods Enzymol. 114*, 452–472.

Husain, M., & Davidson, V. L. (1985) *J. Biol. Chem. 260*, 14626–14629.

Husain, M., & Davidson, V. L. (1986) *J. Biol. Chem. 261*, 8577–8580.

Husain, M., & Davidson, V. L. (1987) *J. Bacteriol. 169*, 1712–1717.

Ishii, Y., Hase, T., Fukumori, Y., Matsubara, H., & Tobari, J. (1983) *J. Biochem. 93*, 107–119.

Kabsch, W., & Sander, C. (1983) *Biopolymers 22*, 2577–2637.

Kumar, M. A., & Davidson, V. L. (1990) *Biochemistry 29*, 5299–5304.

Lommen, A., Canters, G. W., & van Beeumen, J. (1988) *Eur. J. Biochem. 176*, 213–223.

Mathews, F. S., Chen, Z. W., & Bellamy, H. D. (1991) *Biochemistry 30*, 238–247.

McIntire, W. S., Wemmer, D. E., Chistosedov, A., & Lidstrom, M. E. (1991) *Science 252*, 817–824.

Reeke, G. N. (1984) *J. Appl. Crystallogr. 17*, 125–130.

Rossmann, M. G., & Argos, P. (1975) *J. Biol. Chem. 250*, 7525–7532.

Sharma, K. D., Loehr, T. M., Sanders-Loehr, J., Husain, M., & Davidson, V. L. (1988) *J. Biol. Chem. 263*, 3303–3306.

Tronrud, D. E., Monzingo, A. F., & Matthews, B. W. (1987) *Acta Crystallogr. A43*, 489–501.

van Beeumen, J., van Bun, S., Canters, G. W., Lommen, A., & Chothis, C. (1991) *J. Biol. Chem. 266*, 4869–4877.

van der Kamp, M., Floris, R., Hali, F. C., & Canters, G. W. (1991) *J. Am. Chem. Soc. 112*, 907–908.

van Spanning, R. M. J., Wansell, C. W., Reijnders, W. N. M., Oltmann, L. F., & Stouthamer, A. H. (1990) *FEBS Lett. 275*, 217–220.

Vellieux, F. M. D., Huitema, F., Groendijk, H., Kalk, K. H., Frank, J., Jongejan, J. A., Duine, J. A., Petratos, K., Drenth, J., & Hol, W. G. J. (1989) *EMBO J. 8*, 2171–2178.

Vellieux, F. M. D., Kalk, K. H., Drenth, J., & Hol, W. G. J. (1990) *Acta Crystallogr. B46*, 806–823.

Xia, Z. X., & Mathews, F. S. (1990) *J. Mol. Biol. 212*, 837–863.